RAPID COMMUNICATIONS

PHYSICAL REVIEW A VOLUME 38, NUMBER 9 NOVEMBER 1, 1988

Nonlinear pattern and wave-number selection in convecting binary mixtures

Jay Fineberg and Elisha Moses
Department of Nuclear Physics, Weizmann Institute of Science, Rehovot, 76100, Israel

Victor Steinberg
Department of Nuclear Physics, Weizmann Institute of Science, Rehovot, 76100, Israel
and Center for Nonlinear Studies, Los Alamos National Laboratory, Los Alamos, New Mexico 87545
(Received 25 July 1988)

We investigate the transition from weakly nonlinear to nonlinear traveling-wave states. Pattern selection due to a transition from convective to absolute instability conditions is found, in good agreement with theory. While the linear properties depend on the (boundary-dependent) threshold of convection, the weakly nonlinear properties refer back to the threshold of an infinite system.

Considerable efforts have recently been made to understand and identify various spatio-temporal transitions from an unstable state to a coherently oscillating or chaotic state in numerous hydrodynamic flows. Oscillatory convection in binary mixtures as well as a variety of open-flow systems show a transition to spatially developing traveling waves (TW). For these systems a generalized Ginzburg-Landau (GGL) equation can be derived as a simple model describing the nonlinear evolution of propagating patterns:[1]

$$\tau_0(\partial_t + s\partial_x)A = (1+ic_0)\epsilon A + (1+ic_1)\xi_0^2\partial_x^2 A - g(1+ic_2)|A|^2 A . \quad (1)$$

Here ϵ is the system's control parameter [e.g., $\epsilon=(R-R_c)/R_c$, where R is the Rayleigh number and R_c its threshold value], and τ_0 and ξ_0 are the characteristic time and length, respectively, s is the group velocity, and g, c_0, c_1, and c_2 are real parameters. The complex amplitude $A(x,t)$ describes the spatio-temporal modulation of the marginal waves.

Unlike stationary bifurcations where only an absolute instability can exist, this type of system [with broken O(2) symmetry] can exhibit both convected and absolute types of instabilities.[2] The difference between the two cases is a relative one in the sense that it depends on the choice of the reference frame in which the instability is considered. In the case of an absolute instability the perturbation grows in time at any fixed point in the system despite the fact that the wave packet is displaced downstream. In the case of a convective instability an initial perturbation may be carried away sufficiently fast so that at the initial site the perturbation decays to zero although in a moving frame it grows. Depending on the interrelation between the rate s/ξ_0, at which a perturbation will be swept a distance ξ_0 downstream and the local growth rate τ_0^{-1}, convected or absolute instability conditions will be satisfied. The type of instability will, in turn, determine the type of pattern selected by the system. In general, it was shown[1,3] that for Eq. (1) the solution $A=0$ becomes convectively unstable for $0<\epsilon<\epsilon_t$, and absolutely unstable for $\epsilon>\epsilon_t$, where $\epsilon_t=(s\tau_0/2\xi_0)^2(1+c_1^2)^{-1}$. The transition from convected to absolutely unstable conditions, in the framework of the GGL equation, occurs at $s_t^*=2(1+c_1^2)^{1/2}$ where $s^*=(s\tau_0/\xi_0)\epsilon^{-1/2}$ is the nondimensional group velocity.[1,3] The selected wave number k^* and frequency ω^* behind the front are[1]

$$k^* = \left[\frac{(1+c_1^2)^{1/2} \pm (1+c_2^2)^{1/2}}{(c_1-c_2)}\right]\frac{\epsilon^{1/2}}{\xi_0} \quad (2)$$

and

$$\omega^* = \tau_0^{-1}(c_0-c_1)\epsilon , \quad (3)$$

where k^* and ω^* are the deviations from the critical values k_c and ω_0, respectively.

Cross[4,5] used this idea of pattern translation to explain the variety of one-dimensional (1D) TW patterns observed in a finite container. He conjectured and showed by numerical simulations of two coupled GGL for left and right going TW, that for $s^*<2$ the nature of the steady solution in finite geometry cells changes from spatially modulated TW (confined TW) to TW that have a saturated value along the entire cell length (full TW). Moreover, for larger values of s^*, spatially and temporally modulated TW can be observed[5] such that most of the complicated experimental patterns[6-9] of 1D TW in convecting binary mixtures can be explained by this model.

Another success of the Cross theory[4] is a complete quantitative description of the dynamical and spatial structure of the linear oscillatory transients in a convective binary mixture in a cell of finite lateral size. A result of this model is a shift in the onset of the Hopf bifurcation ϵ_s that is inversely proportional to the length of the container L, and is due to the reflection of the TW at the lateral boundaries. Recent experiments quantitatively confirm most of the theoretical predictions in the linear regime[10,11] as well as the sequence of nonlinear patterns selected.[6-9] Quantitative verification of the nonlinear properties observed in numerical simulations of the model and the influence of thermal boundary conditions at the lateral walls on linear and nonlinear solutions have not been performed to date. This is the subject of the paper presented.

In a binary fluid, the parameters which determine the convective flow are the Rayleigh number R, which is the nondimensional temperature difference ΔT across the fluid layer, and the separation ratio ψ, which is a measure of coupling between temperature and concentration gradients induced by Soret effect.[12] It is the sign and the value of ψ that determine if the convective state is oscillatory or stationary. For $\psi<0$ the concentration gradient stabilizes the conduction state, as the imposed temperature gradient destabilizes it. Their competition gives rise to a Hopf bifurcation at R_c.[12] Other relevant dimensionless parameters are the Prandtl number $P=\nu/\kappa$ and Lewis number $\mathcal{L}=D/\kappa$ where ν is the kinematic viscosity, D and κ are the mass and thermal diffusivities, respectively.

Our measurements reveal the following basic features of the nonlinear regime: (i) The value of the temperature difference ΔT_∞ obtained by interpolation of convective heat-transport measurements (Nusselt number N vs ΔT) for the saturated TW branch till the intersection with the $N=1$ axis, coincides with the threshold for oscillatory convection in an infinite container. The absolute value of the onset shift ϵ_s from ΔT_∞ due to the finite geometry of the cell is in quantitative agreement with the theory.[4] (ii) We quantitatively confirm the criterion for the transition from weakly nonlinear confined TW to full TW pattern at ϵ_t in a wide range of ψ. (iii) The nonlinear properties of the confined TW (heat transport and propagation velocity) are not altered when thermal boundary conditions at the lateral walls are varied although the convection onset is shifted. (iv) Due to boundary effects, the confined TW branch is hidden for $\psi>\psi^*$ (where ψ^* is determined by $\epsilon_s\geq\epsilon_t$). (v) Selection of the average wave number k of the confined TW branch is observed. The frequency of confined TW decreases linearly with ϵ.

Our experiments were done on ethanol-water mixtures with weight concentrations ranging between 25.5–28.5%. ψ ranges between -0.005 and -0.078, $P\approx 18$, and $\mathcal{L}\approx 0.01$. We used cells constructed of both high-density polyethylene (HDPE) with thermal conductivity $\lambda=5$ mW/cm K and polypropylene (PP) ($\lambda=1.2$ mW/cm K) with heights $d=0.3$ cm and 0.305 cm, respectively. A PP cell with metal or HDPE strips glued to its endwalls was also used in order to vary their thermal conductivity. Experiments were performed with cells of aspect ratios $1:4:\Gamma$ where $\Gamma=12$ and 20. Our experimental apparatus is described elsewhere.[6]

Typical heat-flow measurements for confined (lower) and saturated TW (upper) branches for $\psi=-0.031$ are presented in Fig. 1 together with a quadratic fit (solid line) of $N-1$ as a function of $(\Delta T-\Delta T_\infty)/\Delta T_\infty$ for the heat transport by saturated TW, where ΔT_∞ is a free parameter (this fit corresponds to a fifth-order amplitude equation). We found that in a wide range of ψ the fit gives values of ΔT_∞ which coincide with the onset value for an infinite system as predicted by linear stability analysis.[13] We *conjecture* that ΔT_∞ corresponds to the critical-temperature difference for the onset of the oscillatory instability in an infinite container. The onset shift ϵ_s predicted by Cross[4] is given by $\epsilon_s=-\ln|r|(s\tau_0/L)$, where r is the reflection coefficient of TW at the lateral walls. Assuming r to be independent[11] of ψ and depending only on the ratio $\lambda_{\text{wall}}/\lambda_{\text{fluid}}$ ($r=0.094$, 0.15, 0.22, for metal, HDPE, and PP, respectively, in reasonable agreement with the theoretically predicted values), we use its value determined by a particular set of data to compare ϵ_s with $\epsilon_{s(\text{expt})}\equiv(\Delta T_c-\Delta T_\infty)/\Delta T_\infty$ (where ΔT_c is the experimentally measured critical temperature difference across the cell) in the inset of Fig. 1. (The points without error bars are obtained by fitting relatively few data points so that the error bars are large). The good agreement between experiment and theory thereby supports our conjecture on the role of ΔT_∞.

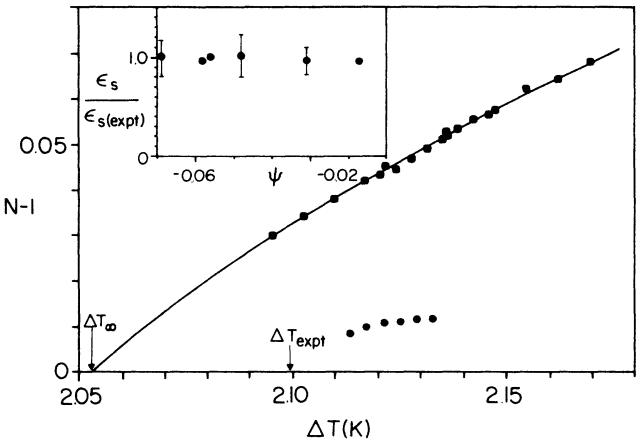

FIG. 1. $N-1$ as a function of ΔT for $\psi=-0.031$. Solid line is a nonlinear fit to the data. Circles, confined TW; squares, full TW. In the inset the ratio of $\epsilon_s/\epsilon_{s(\text{expt})}$ as a function of ψ is presented.

The influence of different thermal boundary conditions at lateral walls on linear and nonlinear behavior of the oscillatory convection is demonstrated in Fig. 2(a). Heat-flow measurements for three cells constructed from PP with PP, HDPE, and metal end walls at the same value of $\psi=-0.058$ are presented on an $N-1$ vs ΔT plot. We observed the following basic features: (a) Varying the boundary conditions at the lateral walls from poor (PP) to good (metal) conductors shifts the oscillatory instability onset due to the variation of the reflection coefficient. The range of the confined TW branch remains unchanged by increasing the hysteretic region. The experimental values of the shift are in quantitative agreement with the theory.[4] (b) The heat transport of the nonlinear TW remains unchanged for different lateral boundaries, and the transition to the next nonlinear state occurs at the same value ΔT_t. (c) The full TW branch does not exist for highly conductive boundaries. This may be due to a pinning of the TW at the wall. The stationary convection branch for the cell with the low-λ (PP) and medium-λ (HPDE) walls coincide with that of the metal-walled cell until losing stability to the full TW branch at the same point. The stationary convection branch for the cell with metal walls extends down to the vicinity of ΔT_∞. After losing stability at a saddle node the system returns to approximately ΔT_∞. We would like to emphasize here that the stationary branch definitely differs from the branch corresponding to full TW as seen from Fig. 2(a).

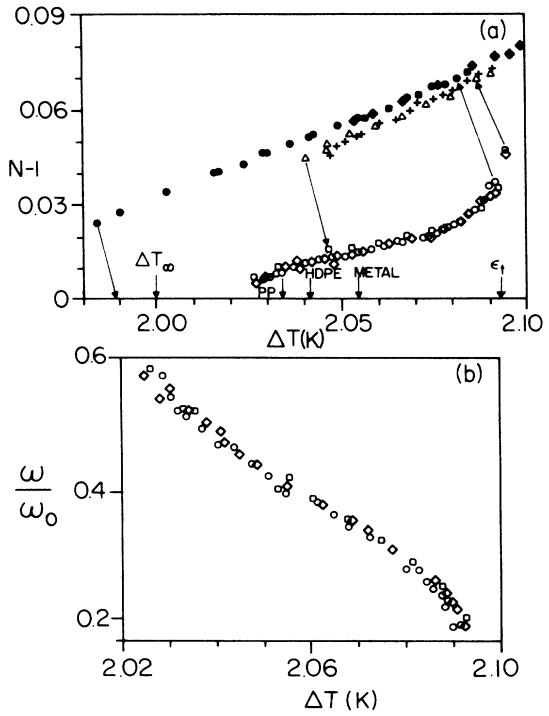

FIG. 2. (a) $N-1$ measurements as a function of ΔT for $\psi=-0.058$ for cells with different lateral walls (squares, PP; diamonds, HDPE; circles, metal walls; open symbols, confined TW; solid symbols, stationary convection; triangles, full TW for PP walls; crosses, full TW for HDPE walls). (b) Frequency ratio ω/ω_0 as a function of ϵ for confined TW at $\psi=-0.058$. $\omega_0=4.9$ is the neutral frequency.

Figure 2(b) shows the dependence of the frequency ω of the confined TW on ΔT for the same values of parameters as in Fig. 2(a). We see that the frequencies along the confined branch for the three sets of data are identical. We obtain for the slope $\partial\omega/\partial\epsilon$ a value of $10.87\omega_0$ which is about order of magnitude larger than predicted by Eq. (3) at $\psi=-0.058$. Thus we observe that for weakly nonlinear TW both the frequencies and heat transport are

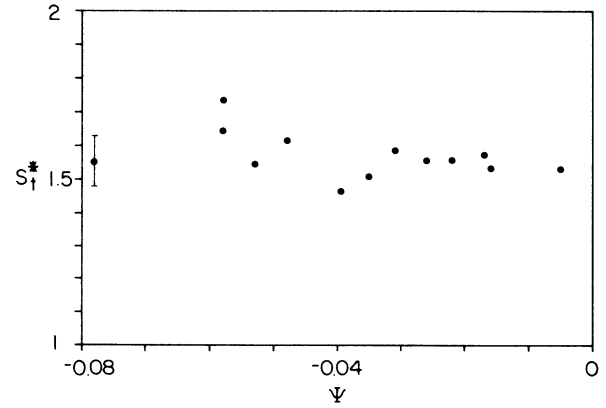

FIG. 3. Nondimensional group velocity of TW at transition from confined to full TW, s_t^*, as a function of ψ. A typical error bar is shown.

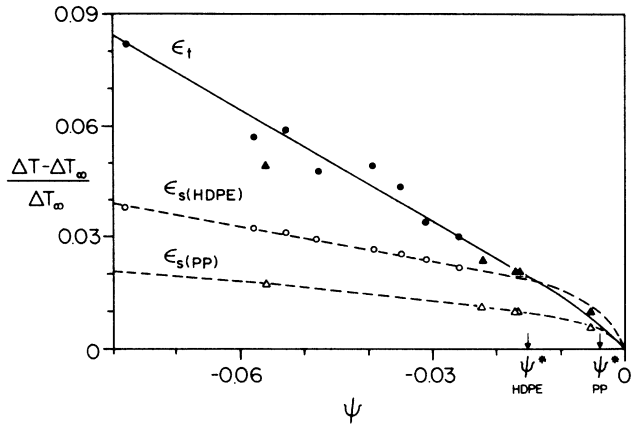

FIG. 4. Region of existence of weakly nonlinear TW in the ϵ-ψ plane for $\Gamma=12$ and boundary conditions using poor and good conductors.

unaffected by variations in lateral boundary conditions. This conclusion is also supported by experiments performed in cells made of HDPE having different aspect ratios for the same value of ψ.

In a previous publication (Moses, Fineberg, and Steinberg[6]) we reported preliminary results on the experimental test of the criterion s_t^*, for the transition from confined to full TW. Here we present quantitative verification of this prediction. The experimental results in the range of ψ between -0.005 and -0.078 are presented in Fig. 3. The experimental value for s_t^* at which the transition occurs is independent of ψ as predicted and is equal to 1.57 ± 0.07. The parameter ξ_0 which appears in formula for s^* was taken from theoretical estimates.[13] Values for τ_0 are the result of interpolation of our experimental measurements, and ϵ_t was obtained using the experimental values ΔT_t and ΔT_∞. We used the value of s in the linear regime[13] as required by marginal stability.[1] Since the observed bifurcation to confined TW is subcritical unlike the supercritical one assumed in Eq. (1), one cannot expect exact quantitative agreement with the value s_t^* predicted but the existence of a sharp selection criterion is indeed apparent.

As an extension of the ideas presented, we find that the

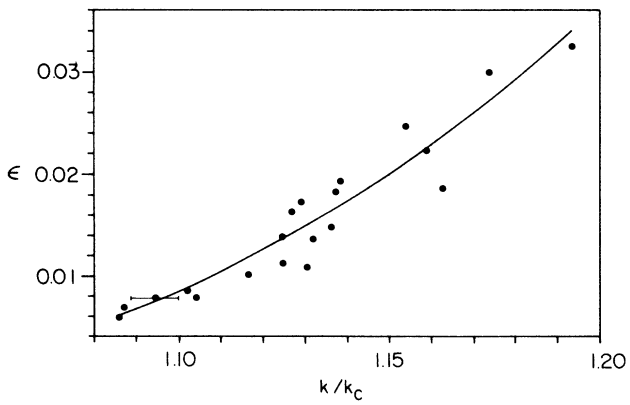

FIG. 5. Dependence of average k/k_c as a function of ϵ at $\psi=-0.058$, $\Gamma=20$, typical error bar shown.

region of the ϵ-ψ plane in which the confined TW branch is observed can be limited by lateral boundary effects. Although the transition to full TW ϵ_t is solely a function of ψ, the onset shift ϵ_s is dependent on both ψ and the lateral boundary conditions [Fig. 2(a)]. Therefore, for given boundary conditions, a value ψ^* exists for which $\epsilon_t = \epsilon_s$. For values of $\epsilon_s > \epsilon_t$ the convection onset will occur in the region where the confined TW branch is already unstable. The transition will then be to a higher branch. Since the saddle node of higher branches in the region of the codimension-2 point extend below that of the confined branch, this branch may be entirely hidden. Figure 4 shows theoretical calculations of both ϵ_s and ϵ_t for poor (PP) and good (HPDE) conductors for aspect ratio $\Gamma = 12$ together with the experimental data. The values ψ^*_{PP} and ψ^*_{HDPE} shown (arrows in Fig. 4) are the least negative values of ψ for which confined TW were *not* observed experimentally for PP and HDPE walled cells (for $\Gamma = 12$), respectively. These points are in remarkably good agreement with the values of ψ for which $\epsilon_s = \epsilon_t$ as seen from the graph.

Another possible consequence of a convected instability condition is the experimentally observed wave-number selection on the confined TW branch. The selection in this dynamical situation may be due to the same mechanism as in the case of vortex-front propagation in Rayleigh-Benard convection.[1,14,15] In Fig. 5 we present the average value of the wave number k/k_c as a function of $\epsilon = (\Delta T - \Delta T_{c(\mathrm{expt})})/\Delta T_{c(\mathrm{expt})}$ along the confined TW branch together with a fit (solid line) of the data to $k/k_c - 1 = (0.405 \pm 0.03)\epsilon^{1/2}\xi_0^{-1}$ ($k_c = 2.98 \pm 0.04$ is the critical value of the wave number obtained from the fit). Using $c_2 = -5.6$ (Ref. 16) and $c_1 = -0.049$ (Ref. 13) one finds from (2) that $k/k_c - 1 = 0.28\epsilon^{1/2}\xi_0^{-1}$. Thus, even though expressions (2) and (3) predict the observed ϵ dependence, we do not find quantitative agreement with the theory.

We thank M. Cross for helpful discussions. This work was supported in part by the U.S. Israel Binational Science Foundation Grant No. 8400256, and the Minerva Foundation.

[1]K. Nozaki and N. Bekki, Phys. Rev. Lett. **51**, 2171 (1983).

[2]L. D. Landau and E. M. Lifshitz, *Hydrodynamics* (Pergamon, London, 1987), Vol. VI.

[3]P. Huerre, in *Instabilities and Nonequilibrium Structures,* edited by E. Tirapegi and D. Villarroel (Reidel, Dordrecht, 1987), p 141; J. M. Chomaz, P. Huerre, and L. G. Redekopp, Phys. Rev. Lett. **60**, 25 (1988).

[4]M. Cross, Phys. Rev. Lett. **57**, 2935 (1987).

[5]M. Cross, Phys. Rev. A **38**, 3593 (1988).

[6]E. Moses and V. Steinberg, Phys. Rev. A **34**, 693 (1986); V. Steinberg and E. Moses, in *Patterns, Defects, and Microstructures in Nonequilibrium,* edited by D. Walgraef, Advanced Study Institute (Martinus Nijhoff, Hingram, MA, 1987), pp. 309–335; E. Moses, J. Fineberg, and V. Steinberg, Phys. Rev. A **35**, 2757 (1987); V. Steinberg, E. Moses, and J. Fineberg, Nucl. Phys. (Proc. Suppl.) **B2**, 109 (1987).

[7]R. Heinrichs, G. Ahlers, and D. S. Cannell, Phys. Rev. A **35**, 2761 (1987); G. Ahlers, D. S. Cannell, and R. Heinrichs, Nucl. Phys. (Proc. Suppl.) **B2**, 77 (1987).

[8]J. Fineberg, E. Moses, and V. Steinberg, Phys. Rev. Lett. **61**, 838 (1988).

[9]P. Kolodner and C. Surko, Phys. Rev. Lett. **61**, 842 (1988).

[10]P. Kolodner, A. Passner, C. Surko, and R. Walden, Phys. Rev. Lett. **56**, 2621 (1986).

[11]C. Surko and P. Kolodner, Phys. Rev. Lett. **58**, 2055 (1987).

[12]D. T. J. Hurle and F. Jakeman, J. Fluid Mech. **47**, 667 (1971); V. Steinberg, J. Appl. Math. Mech. **35**, 335 (1971).

[13]M. Cross and K. Kim, Phys. Rev. A **37**, 3909 (1988).

[14]G. Dee and J. S. Langer, Phys. Rev. Lett. **50**, 383 (1985).

[15]J. Fineberg and V. Steinberg, Phys. Rev. Lett. **58**, 1332 (1987).

[16]Wolfgang Schopf, M.Sc. thesis, University of Bayreuth, Germany, 1988 (unpublished).